Catalysis Science & Technology

Accepted Manuscript

This article can be cited before page numbers have been issued, to do this please use: A. Tanaka, T. Okamoto and H. Kominami, *Catal. Sci. Technol.*, 2026, DOI: 10.1039/D6CY00446F.

ROYAL SOCIETY OF CHEMISTRY

rsc.li/catalysis

View Article Online
DOI: 10.1039/D6CY00446F

ARTICLE

Visible-light-driven hydrogenation of styrene via plasmon-induced H_2 dissociation on Au/ZrO_2 catalysts

Received 00th January 20xx,
Accepted 00th January 20xx

DOI: 10.1039/x0xx00000x

Atsuhiro Tanaka,* Tamaki Okamoto and Hiroshi Kominami *

Herein, we report the visible-light-driven hydrogenation of styrene using a supported gold (Au) particle catalyst. Various metal oxides (MOx: TiO_2, SiO_2, ZrO_2, and CeO_2) were investigated as support materials to elucidate the role of the metal-semiconductor interface in plasmon-induced charge separation and catalytic activity. Au/ZrO_2 exhibited the highest activity, producing ethylbenzene with a turnover number of 12. Characterization techniques, including XPS, UV-vis spectroscopy, and TEM, confirmed the presence of metallic Au nanoparticles with an average size of 6.8 nm on the ZrO_2 support. Action spectrum and light intensity dependence studies revealed that the reaction was driven by the surface plasmon resonance of Au nanoparticles rather than thermal activation. In situ DRIFT spectroscopy detected the formation of Au-H species under visible-light irradiation, confirming the dissociative adsorption of H_2 on the Au surface. Kinetic isotope effect analysis using H_2 and D_2 yielded an exceptionally large k_H/k_D value of 22, suggesting that the dissociative adsorption of H_2 is the rate-determining step. A catalytic cycle involving hot electron injection into the antibonding orbital of H_2 was proposed. These findings provide mechanistic insights into plasmon-induced hydrogenation on Au nanoparticles and demonstrate the potential of sustainable and selective catalytic systems.

1. Introduction

The hydrogenation of unsaturated hydrocarbons, such as alkenes and alkynes, plays a pivotal role in the fine chemical and petrochemical industries. Typically, these reactions are catalyzed by transition metals such as palladium (Pd), platinum (Pt), and nickel (Ni). According to the Sabatier principle, these metal surfaces possess moderate adsorption energies for molecular hydrogen (H_2), allowing for the facile dissociation of H_2 driven by thermal energy to form active surface hydrogen species (M-H), thereby promoting the reaction[1].

Although gold (Au) was historically considered inert, its catalytic properties, particularly when dispersed as nanoparticles, have garnered significant attention. This includes its exceptional activity for CO oxidation[2] and its utility in organic syntheses, such as the chemoselective hydrogenation of nitro and carbonyl groups[3]. Despite these advances, the hydrogenation of simple alkenes (C=C bonds) using Au catalysts remains challenging, often exhibiting significantly lower activity than traditional Pd or Pt catalysts. Density functional theory (DFT) calculations have attributed this to the high activation barrier for the dissociative adsorption of H_2 on Au surfaces (approximately 0.5 eV or higher on the Au(111) facet)[4,5]. Therefore, historically, high thermal energy or a specialized activation mechanism has been required to activate H_2 on Au particles.

Recently, photocatalytic reactions utilizing the surface plasmon resonance (SPR) of metal particles, often coupled with semiconductor supports, have garnered significant attention as a strategy to overcome the high energy barrier for H_2 dissociation on Au surfaces. The choice of support material, such as various metal oxides (MO_x), can significantly influence charge separation and the overall efficiency of plasmon-induced processes, making systematic investigations crucial. Upon the absorption of visible light by Au particles, collective electron oscillations are excited, and the subsequent non-radiative decay of these plasmons generates energetic hot electrons[6]. Mukherjee et al. experimentally and theoretically demonstrated that the injection of these hot electrons into antibonding orbitals at the Au surface enables the dissociation of H_2 molecules even at room temperature[7]. Furthermore, phenomena such as H-D formation via H_2 and deuterium (D_2) exchange reactions utilizing these generated active species have been reported[8], suggesting that plasmon excitation can access reaction pathways distinct from those governed by thermal equilibrium. However, most prior studies have focused on the decomposition or exchange of simple molecules. There are few examples of the successful application of plasmon-induced H_2 dissociation in the synthesis of organic molecules, such as ethylbenzene, while providing a detailed elucidation of the reaction mechanism and kinetic behavior, particularly regarding the spectroscopic observation of intermediates and isotope effects.

Herein, we report the hydrogenation of styrene using supported Au particle catalysts under visible-light irradiation. First, we investigated the influence of various metal oxide supports (e.g., ZrO_2 and TiO_2) on plasmon-induced charge

[a] Department of Applied Chemistry, Faculty of Science and Engineering, Kindai University, Kowakae, Higashiosaka, Osaka 577-8502, Japan

† Footnotes relating to the title and/or authors should appear here.

separation and catalytic activity to elucidate the role of the metal-semiconductor interface. Second, to demonstrate that the reaction was driven by plasmonic excitation rather than thermal activation, the action spectra (wavelength dependence) and light intensity dependence were analyzed. Furthermore, to gain molecular-level insights into the reaction mechanism, we employed in situ DRIFT spectroscopy to monitor the surface adsorbates and conducted kinetic isotope effect (KIE) analysis using H_2 and D_2 gas. Based on these approaches, we discuss the mechanism of H_2 activation and the rate-determining step of plasmon-induced hydrogenation on Au particles.

2. Experimental section

2-1. Preparation of Au/MO_x

Titanium(IV) oxide (TiO_2, ST-01, Ishihara Sangyo), zirconium(IV) oxide (ZrO_2, Kanto Chemical), silicon(IV) oxide (SiO_2, Kanto Chemical), and cerium(IV) oxide (CeO_2, Nanotek, Kanto Chemical) were used as metal oxides (MO_x) for the support material, which was pretreated by calcination at 600°C for 1 h in air. The specific surface areas of the samples after preliminary calcination were as follows: ZrO_2 (4 $m^2\ g^{-1}$), TiO_2 (15 $m^2\ g^{-1}$), SiO_2 (12 $m^2\ g^{-1}$) and CeO_2 (7 $m^2\ g^{-1}$). Au-supported MO_x (Au/MO_x) was prepared using a precipitation method[9]. Sodium hydroxide solution (1 mol dm^{-3}) was added to 100 cm^3 of gold chloride aqueous solution (0.078 mmol dm^{-3}) until the pH reached 10, and then pre-calcined MO_x (1.0 g) was suspended in the solution. This suspension was stirred at room temperature for 20 min, and then at 343 K for 2 h. The suspension was then cooled to room temperature, filtered, washed with distilled water (500 cm^3), and vacuum-dried at 298 K for 2 h. The dried powder was heat-treated at 523 K for 1 h in a tubular furnace while flowing H_2 gas through it. The H_2 gas flow rate was set at 70 $cm^3\ min^{-1}$.

2-2. Characterization of catalysts

The diffuse reflectance spectra of the Au/MO_x samples were obtained using a UV-visible spectrometer (UV-2600, Shimadzu, Kyoto, Japana) equipped with a diffuse reflectance measurement unit (ISR-2600Plus, Shimadzu). The morphologies of the samples were observed using a JEOL JEM-2100F transmission electron microscope (TEM) operated at 200 kV at the Joint Research Center of Kindai University. To observe the electronic states of Au on the catalyst surface, measurements were performed using an X-ray photoelectron spectrometer (PHI VersaProbe 4, ULVAC-PHI, Kanagawa, Japan). The sample was then analyzed in 0.1 eV steps using Al Kα radiation within a vacuum chamber, with a binding energy correction applied at C 1s (284.6 eV). In situ diffuse reflectance infrared Fourier transform (DRIFT) spectra were measured using an FT-IR spectrometer (FT/IR-6600, JASCO, Tokyo, Japan) equipped with a mercury cadmium tellurium (MCT) detector cooled by liquid nitrogen at a resolution of 1 cm^{-1}. The sample powder was placed in a diffuse reflectance cell, which was fitted by a potassium bromide (KBr) window at the top. The background spectrum was measured after the pretreatment under a N_2 gas flow at the 323 K.

2-3. Hydrogenation of styrene

The dried photocatalyst powder (50 mg) was suspended in an acetonitrile solution (5 cm^3) containing 30 µmol of styrene as a substrate in a test tube. The mixture was bubbled with H_2, and sealed with a rubber septum. The suspension was irradiated with visible light from a green LED (KPI, Hyogo, Japan) while stirring magnetically at 293 K. The reaction mixture was filtered through a syringe filter, and the liquid phase was analyzed using GC-2025 (FID-type detector with a DB-1 column, Shimadzu).

2-4. Isotope effect in the hydrogenation of styrene

The reaction conditions were the same as those described in 2-3 above. The system was substituted with deuterium. The post-reaction liquid phase was analyzed using a gas chromatography-mass spectrometer (GC-MS) equipped with a DB-1 column (Shimadzu).

3. Results and discussion

3-1. Effects of various metal oxides as materials for stabilizing Au particles

Various metal oxides (MO_x: TiO_2, SiO_2, ZrO_2, and CeO_2) were examined as materials for stabilizing Au particles. The results of the hydrogenation reaction of styrene (ST) to ethylbenzene (EB) using Au/MO_x supported on various metal oxides under green LED irradiation and in the dark are shown in Figure 1. In all cases, the amount of product formed under green LED irradiation significantly exceeded that formed in the dark, suggesting that the reaction proceeded via light-induced hydrogen dissociation. In all cases, the selectivity for the produced EB was over 99%, indicating that the observed differences among the supports reflected the differences in their reaction rates. Notably, when MOx was used without Au particles as a catalyst, hydrogenation of ST did not occur in any case, and no EB was produced.

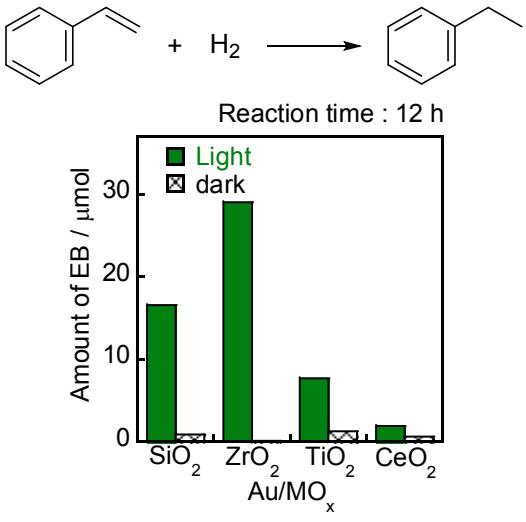

View Article Online
DOI: 10.1039/C6CY01465F

Figure 1 The effect of kinds of support of Au on hydrogenation of styrene to ethylbenzene under irradiation of visible light from green LED.

Thus, the hydrogenation reaction accompanied by hydrogen dissociation under visible-light irradiation was induced by Au particles. Among the catalysts, Au/ZrO_2 produced the highest amount of EB.

3-2 Characterization of Au/ZrO_2

Figure 2 shows the XPS, UV-vis, TEM, and size distribution of Au particle for Au/ZrO_2, which exhibited the highest activity among the investigated supports. The Au 4f XPS spectra of the samples are shown in Figure 2a. As previously reported[10], the as-prepared (uncalcined) sample exhibited peaks attributable to $Au(OH)_3$ in its XPS spectrum. After reduction via calcination under H_2 flow, the sample exhibited two peaks at 83.3 and 86.9 eV, respectively.

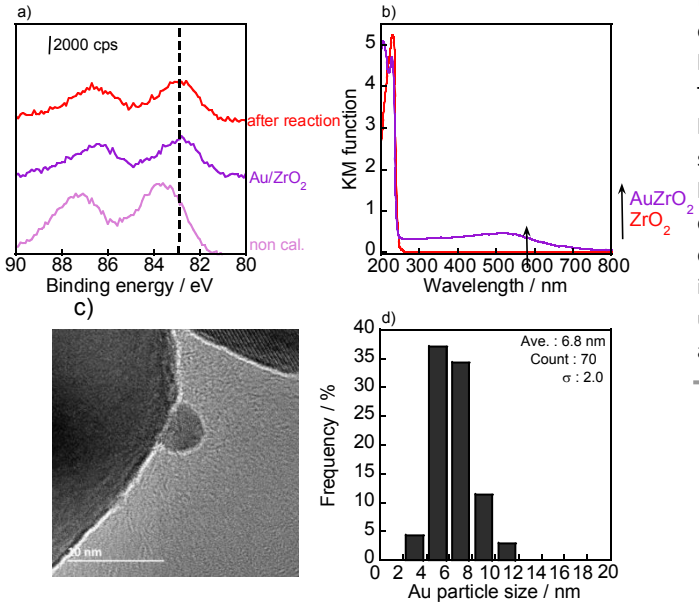

Figure 2 (a) XPS spectra of various Au/ZrO_2 samples around Au 4f component, (b) UV-vis spectra of ZrO_2 and Au/ZrO_2, (c) TEM photograph and (d) Au particle size distribution of Au/ZrO_2.

These binding energies matched the peak positions obtained from the XPS data of the gold foil (Figure S1), confirming that the supported gold was in the metallic state (Au^0). Furthermore, the XPS spectrum of the post-reaction sample showed no change compared to the pre-reaction (calcined) sample, indicating that the metallic Au state was retained after the reaction. From this, we concluded that the Au particles remained stable (or did not undergo any changes) during the hydrogenation reaction in the H_2 atmosphere. Figure 2b shows the photoabsorption properties of ZrO_2 and Au/ZrO_2. The unmodified ZrO_2 sample exhibited absorption only at $\lambda < 250$ nm, corresponding to a bandgap of 5.0 eV. In the Au/ZrO_2 spectrum, strong light absorption was observed at approximately 550 nm, which was attributed to SPR of the supported Au particles. The UV-vis spectra of the Au/MO_x powders, discussed in Figure 1, are shown in Figure S2, all these samples exhibited absorption due to Au SPR. Figure 2c shows a TEM image of Au/ZrO_2, confirming the deposition of Au particles on the ZrO_2 support. The corresponding particle size distribution (Figure 2d), derived from TEM, indicates an average Au particle size of 6.8 nm. The TEM images of all Au/MO_x samples (Figure S3) show Au particles smaller than 10 nm. Although the average Au particle size on ZrO_2 (6.8 nm) was larger than that on SiO_2 (3.5 nm), Au/ZrO_2 exhibited much higher catalytic activity. In general thermocatalysis, smaller particles are favorable because of their larger surface area. However, in our plasmon-driven system, larger Au particles within this size range can absorb visible light more strongly via SPR, generating more hot electrons. In addition, compared to a highly inert oxide like SiO_2, ZrO_2 provides a more favorable metal-support interface that can serve as an extended reaction field. Therefore, the Au particle size was not the determining factor for hydrogenation activity. The electron transfer behavior from Au to the MO_x support is crucial, as electrons generated on Au particles are known to transfer to MO_x with a conduction band potential more positive than -0.61 V vs. NHE[11], such as TiO_2 and CeO_2. This electron transfer to the support prevents hot electrons from being utilized for H_2 dissociation on the Au surface. In contrast, ZrO_2 has a much more negative conduction band potential, which blocks the transfer of hot electrons to the conduction band. Therefore, the hot electrons remained confined within the Au particles and were efficiently injected into the antibonding orbital of the adsorbed H_2. This efficient utilization of hot electrons explains why Au/ZrO_2 exhibits higher activity than the other metal oxides.

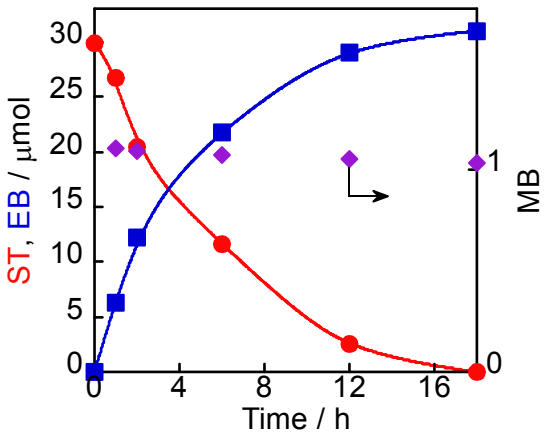

Figure 3 Time courses of amounts of styrene (●), ethylbenzene (■) and material balance (◆) in acetonitrile suspension of Au/ZrO_2 under an H_2 atmosphere and irradiation of visible light from a green LED.

3-3 Time course of hydrogenation reaction of styrene over Au/ZrO_2

Figure 3 shows the time course of the hydrogenation of ST over Au/ZrO_2 at 293 K under visible-light irradiation from a green LED. The figure shows the amounts of ST, EB, and material

View Article Online
DOI: 10.1039/D6CY00446E

balance (MB) plotted against the irradiation time. The equation used to calculate the MB is as follows:

$$\text{Material balance} = (nST + nEB)/n_0ST$$

As the irradiation time increased, the substrate (ST) was consumed, and the formation of EB was confirmed. The MB was maintained at all time points, and the reaction was completed after 18 h of light irradiation. The amount of EB produced after 18 h (30 µmol) exceeded the amount of Au loaded onto the catalyst (2.5 µmol). The turnover number (TON) calculated from this result was 12. This indicates that the hydrogenation of ST under these irradiation conditions is a catalytic reaction rather than a stoichiometric reaction between Au and ST.

The effects of various conditions on the hydrogenation of ST to EB over Au/ZrO_2 were investigated, and the results are summarized in Table 1. Under visible light irradiation from a green LED, the hydrogenation reaction proceeded over Au/ZrO_2 (entry 1). After 12 h of light irradiation, 29 µmol of EB was produced. In contrast, negligible EB was formed (0.34 µmol) under dark conditions (entry 2). This suggests that a thermal reaction did not occur on the Au catalyst surface. Furthermore, hydrogenation did not occur in the absence of H_2 (entry 3) or Au particles in the catalyst (entry 4). These results indicate that visible-light irradiation, Au particles, and the addition of H_2 are indispensable for this reaction.

Table 1 The amount of ethylbenzene in acetonitrile suspensions of various samples under Ar or H_2 atmosphere under dark or irradiation of visible light from green LED.

Entry	Cat.	Atm.	Light	EB / µmol
1	Au/ZrO_2	H_2	on	29
2	Au/ZrO_2	H_2	off	0.34
3	Au/ZrO_2	Ar	on	n.d.
4	ZrO_2	H_2	on	n.d.

3-4 Wavelength dependence

To determine whether this reaction proceeds via the induction of Au SPR rather than by Au thermocatalytic action or local heating of the metal particles under light irradiation, the wavelength dependence was investigated. The action spectrum for this reaction system was obtained by performing the hydrogenation of ST over Au/ZrO_2 at 298 K under visible-light irradiation from a monochromated Xe lamp with a 20 nm bandwidth. The apparent quantum efficiency (AQE) for each central wavelength was calculated using equation (1):

AQE = (rate of ethylbenzene formation/rate of incident photons) × 100

The action spectrum was obtained by plotting the AQE against the wavelength of the incident monochromatic light in the 400-700 nm range. The results are shown in Figure 4. A photoabsorption peak originating from the SPR of the Au particles was observed at approximately 550 nm, and the action spectrum exhibited a trend that correlated well with the photoabsorption. This indicates that the reaction proceeded via light absorption, which was attributed to the SPR of the Au particles. Furthermore, in this experiment, an AQE exceeding 1.3% was achieved upon irradiation with light corresponding to SPR.

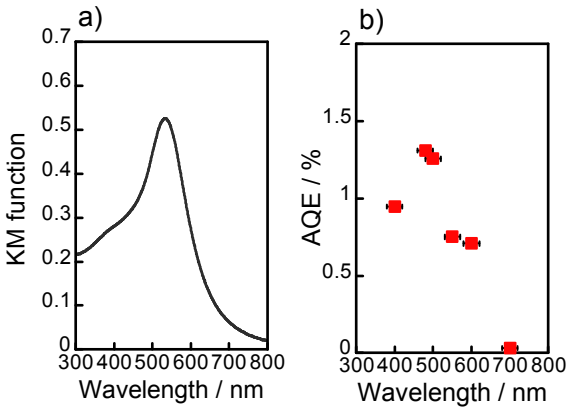

Figure 4 (a) Absorption spectrum of Au/ZrO_2 and (b) action spectrum of Au/ZrO_2 in hydrogenation of ST to EB.

3-5 Observation of hydrogen dissociation species using DRIFT

The dissociated hydrogen species (Au-H) generated under light irradiation were investigated using DRIFT spectroscopy. Previous studies have reported that the vibrational band characteristic of Au-H species appears in the range of 2134-2164 cm^{-1} [12]. Figure 5 shows the DRIFT spectra obtained at room temperature in the dark and under irradiation with a green LED. During measurements conducted in the dark at room temperature for 3 h, no specific peaks or spectral changes were observed. In contrast, upon light irradiation, a distinct peak appeared at approximately 2136 cm^{-1}. This peak was attributed to the Au-H species formed via the dissociative adsorption of H_2 on the Au surface. The increase in the peak intensity with the duration of light irradiation corresponded to an increase in the amount of Au-H species generated by light irradiation. These IR measurements successfully detected the Au-H species as a distinct peak, confirming that their formation was induced by light irradiation.

View Article Online
DOI: 10.1039/D6CY00446F

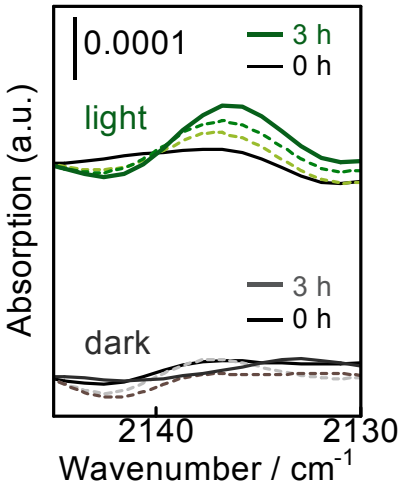

Figure 5 DRIFT spectra of Au/ZrO_2 in H_2 gas for 3 h under the dark and visible light irradiation from a green LED.

3-6 Dependence of light intensity

Having confirmed the light-induced formation of Au-H species via DRIFT, we further investigated the fundamental energy transfer mechanisms driving this photocatalytic activity by examining the dependence of the reaction rate on the light intensity. The dependence of photocatalytic activity on light intensity provides crucial insights into the mechanism of energy transfer from light to surface reactions. Generally, the relationship between catalytic activity and light intensity exhibits three distinct patterns: exponential, linear, and super-linear. First, we consider a case dominated by the "photothermal effect," in which light irradiation induces localized heating within the metal particles. Assuming that the temperature increase is proportional to the light intensity, the reaction rate increases exponentially as the light intensity increases. Wang et al. observed an exponential trend in the carbon monoxide production rate during reduction of carbon dioxide over an Au/ZnO catalyst[13]. A linear relationship between the catalytic activity and light intensity suggests an electron-driven chemical reaction. Mukherjee et al. reported that H-D formation resulting from H_2 and D_2 dissociation on Au particles exhibits this linear dependence[7]. Furthermore, a superlinear relationship indicates that the reaction rate is proportional to I^n (where I is the light intensity and n > 1). Christopher et al. observed a superlinear relationship during ethylene epoxidation on Ag nanocubes[6]. Based on these results, we propose that a superlinear dependence appears when the reaction occurs at "hot spots," where the electromagnetic energy collected by the clusters is efficiently transferred to the adsorbates. Figure 6 shows the effect of light intensity on the reaction rate of ST hydrogenation. Although the reaction rate increased with light intensity, a nonlinear relationship was observed (Figure 6a). However, the double logarithmic plot of the reaction rate versus light intensity (Figure 6b) reveals a linear correlation with a slope of 1.6. This confirms a superlinear relationship in which the reaction rate is proportional to I^n. These results suggest that the observed superlinear behavior arises from a combination of the linear dependence of H_2 dissociation and the promotion of the hydrogenation reaction via "hot spot" formation. This implies that the reaction proceeds via a coupled mechanism involving SPR-induced electron transfer and a photothermal effect.

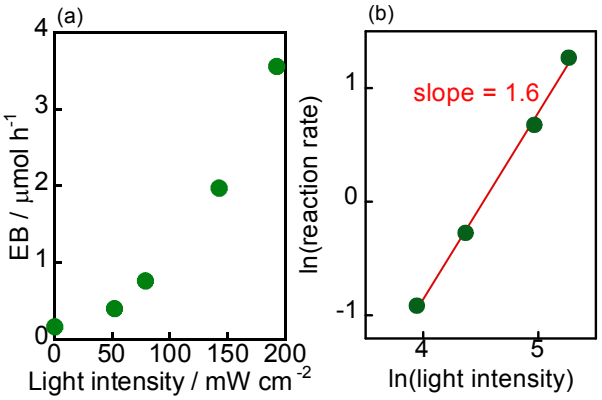

Figure 6 (a) Effect of light intensity on the reaction rate, (b) double logarithm plots of the light intensity and the reaction rate.

3-7 Isotope effect in the hydrogenation of styrene

Figure 7 shows the results of the isotope labeling experiments for the hydrogenation of ST over Au/ZrO_2 using deuterium (D_2) gas. The reactions were conducted at 293 K under an atmosphere of 1 atm of H_2 or D_2. Following the reaction, the liquid phase was separated from the catalyst and analyzed using GC-MS. Figures 7(a) and 7(b) show the mass spectra of EB obtained from the liquid phase after hydrogenation in the presence of H_2 and D_2, respectively. The samples were introduced into the mass spectrometer after separation by gas chromatography using a DB-1 column. In the experiment using H_2 (Figure 7(a)), product peaks were observed at m/z values of 106 and 91. The peak at m/z = 106 was assigned to the molecular ion of the product, EB, corresponding to $[C_8H_{10}]^+$. Additionally, the peak at m/z= 91 represents the base peak ion of EB, which is attributed to the tropylium ion, $[C_7H_7]^+$. This result is consistent with the reference data generated from the mass spectral database of EB provided by the AIST (Figure S4). In contrast, for the experiment using D_2, the retention time in the GC chromatogram remained substantially unchanged. However, in the mass spectrum of the peak identified as EB in the D_2 addition experiment (Figure 7(b)), a signal was observed at m/z= 108. This corresponds to $[C_8H_8D_2]^+$, indicating the addition of D_2 to ST. A concurrent peak observed at m/z= 92 indicates the presence of $[C_7H_6D]^+$. Notably, no peak at m/z= 106 was observed when D_2 was employed. Furthermore, no species corresponding to deuterated ST (m/z = 106) were detected in the mass spectrum of the unreacted ST. The confirmation of EB-d2 as the hydrogenation product in a D_2 atmosphere demonstrates that D_2 is the direct hydrogen source in this reaction. These results suggest that hydrogenation over

View Article Online
DOI: 10.1039/D6CY00446F

Au/ZrO_2 proceeds via hydrogen species dissociated on the Au particles.

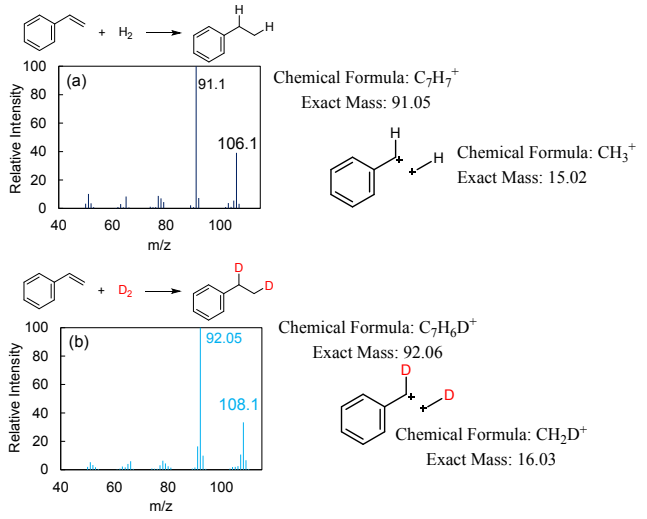

Figure 7 Mass spectra of ethylbenzene in hydrogenation of styrene to ethylbenzene over Au/ZrO_2 under (a) H_2 and (b) D_2 atmosphere under irradiation of visible light from green LED.

Figure S5 shows the time course of ethylbenzene production under green LED irradiation in H_2 and D_2 atmospheres. The respective rate constants are denoted as k_H and k_D. From these results, an exceptionally large kinetic isotope effect (KIE) of $k_H/k_D = 22$ was observed for the hydrogenation of ST. This value significantly exceeds the semiclassical limit (approximately 7) based on simple bond dissociation, suggesting the hydrogen activation cannot be explained by classical models. A similarly massive KIE was reported by Furukawa et al. for ST hydrogenation using specific Rh-based intermetallic compounds, such as $RhPb_2$ ($k_H/k_D = 91$), where the dissociative adsorption of H_2 on a surface densely covered with adsorbed styrene is considered the rate-determining step (RDS) of the reaction[14]. In the present system, it is evident that the dissociative adsorption of molecular hydrogen is the RDS, given that the formation of Au–H species was confirmed by DRIFT measurements only under light irradiation and that the reaction did not proceed in the dark. Furthermore, these kinetic results exclude the possibility of mass transport limitations in the catalytic system. If the overall reaction were limited by the diffusion of substrates (H_2 or styrene) to the catalyst surface, the reaction rate would not exhibit the strong superlinear dependence on light intensity observed in Figure 6, and the KIE would be much smaller (close to the theoretical diffusion limit) than 22. Therefore, the reaction operates strictly under kinetic control.

3-8. Proposed catalytic cycle for styrene hydrogenation over Au/ZrO_2

Based on the current understanding, Figure 8 shows the proposed mechanism for hydrogen dissociation on zirconium oxide supporting Au particles under visible light and the subsequent hydrogenation of styrene using this process. The overall reaction proceeds in six steps:

Step 1: Adsorption of styrene molecules onto the surface of the Au nanoparticles.

Step 2: Excitation of the SPR of Au nanoparticles by visible-light irradiation, generating hot electrons via non-radiative decay.

Step 3: Physisorption of H_2 onto the Au surface.

Step 4: Injection of hot electrons into the σ_u* antibonding orbital of H_2, inducing dissociation via a transient negative ion ($H_2^{\delta-}$) state. The difference in nuclear motion velocities between H and D on the excited-state potential energy surface (PES), arising from their mass difference, leads to an extraordinarily large kinetic isotope effect (KIE).

Step 5: Successive addition of dissociated hydrogen atoms (Au-H) to the vinyl group of the adsorbed styrene.

Step 6: Desorption of the resulting ethylbenzene and regeneration of the active sites on the Au surface.

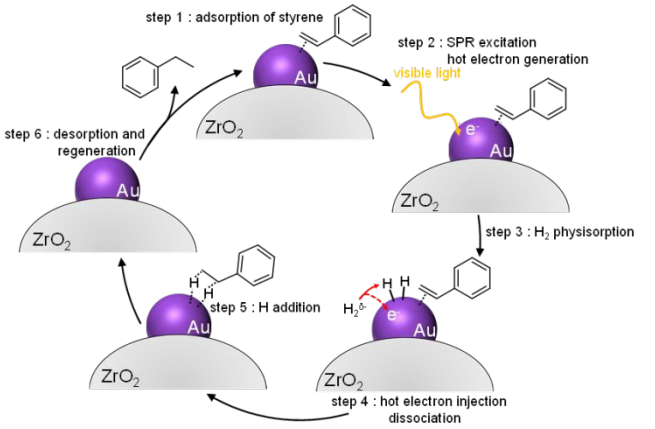

Figure 8 Proposed mechanism of H_2 dissociation and hydrogenation on the surface of Au particles.

Conclusions

This study reports the visible-light-driven hydrogenation of styrene using a supported Au particle catalyst. Various metal oxides have been investigated as support materials, with Au/ZrO_2 exhibiting the highest activity. Characterization techniques confirmed the presence of metallic Au particles with an average size of 6.8 nm on the ZrO_2 support. The reaction was driven by the SPR of the Au particles rather than thermal activation. In situ DRIFT spectroscopy detected the formation of Au-H species under visible-light irradiation, confirming the dissociative adsorption of H_2 on the Au surface. Kinetic isotope effect analysis yielded an exceptionally large value of k_H/k_D= 22, suggesting that the dissociative adsorption of H_2 is the rate-determining step. A catalytic cycle involving hot electron injection into the antibonding orbital of H_2 was proposed. Optimizing H_2 activation via interfacial and structural engineering is crucial for future plasmonic catalyst design. Fine-tuning the metal-support interface to enhance hydrogen spillover and investigating the properties of the support are

important directions for further improving the efficiency of hot electron utilization.

Author contributions

Atsuhiro Tanaka: conceptualization, formal analysis, writing – original draft, review & editing, supervision, funding acquisition, project administration, final approval of the article. Tamaki Okamoto: investigation, acquisition of data, analysis of data, final approval of the article. Hiroshi Kominami: writing – review & editing, supervision, funding acquisition, project administration, final approval of the article.

Conflicts of interest

There are no conflicts to declare.

Data availability

The data supporting this article have been included as part of the ESI. †

Acknowledgements

This work was supported by KAKENHI 22H00274, 23H01767, 23K17964 and 26K01309 from the Japan Society for the Promotion of Science. A. T. is grateful for financial support from Proterial Materials Science Foundation and Yashima Environment Technology Foundation. H. K. expresses gratitude for the financial support from Nippon Sheet Glass Foundation for Materials Science and Engineering.

References

1 A. J. Medford, A. Vojvodic, J. S. Hummelshøj, J. Voss, F. Abild-Pedersen, F. Studt, T. Bligaard, A. Nilsson and J. K. Nørskov, *J. Catal.*, 2015, **328**, 36–42.
2 M. Haruta, T. Kobayashi, H. Sano and N. Yamada, *Chem. Lett.*, 1987, **16**, 405–408.
3 A. Corma and P. Serna, *Science*, 2006, **313**, 332–334.
4 B. Hammer and J. K. Norskov, *Nature*, 1995, **376**, 238–240.
5 M. Wijzenbroek, D. Helstone, J. Meyer and G.-J. Kroes, *J. Chem. Phys.*, 2016, **145**, 144701.
6 P. Christopher, H. Xin and S. Linic, *Nat. Chem.*, 2011, **3**, 467–472.
7 S. Mukherjee, F. Libisch, N. Large, O. Neumann, L. V. Brown, J. Cheng, J. B. Lassiter, E. A. Carter, P. Nordlander and N. J. Halas, *Nano Lett.*, 2013, **13**, 240–247.
8 S. Mukherjee, L. Zhou, A. M. Goodman, N. Large, C. Ayala-Orozco, Y. Zhang, P. Nordlander and N. J. Halas, *J. Am. Chem. Soc.*, 2014, **136**, 64–67.
9 M. Haruta, S. Tsubota, T. Kobayashi, H. Kageyama, M. J. Genet and B. Delmon, *J. Catal.*, 1993, **144**, 175–192.
10 E. Fudo, A. Tanaka and H. Kominami, *ACS Appl. Nano Mater.*, 2022, **5**, 8982–8990.
11 E. Fudo, A. Tanaka and H. Kominami, *Catal. Sci. Technol.*, 2019, **9**, 3047–3054.
12 R. Ju Arez, S. F. Parker, P. Concepci, A. Corma and H. Garc, *Chem. Sci.*, 2010, **1**, 731–738.
13 C. Wang, O. Ranasingha, S. Natesakhawat, P. R. Ohodnicki Jr, M. Andio, J. P. Lewis and C. Matranga, *Nanoscale*, 2013, **5**, 6968–6974.
14 S. Furukawa, P. Yi, Y. Kunisada and K.-I. Shimizu, *Sci. Technol. Adv. Mater.*, 2019, **20**, 805–812.

View Article Online
DOI: 10.1039/D6CY00446F

Data Availability Statement

The data supporting this article have been included as part of the ESI.†